JMEPEG (2011) 20:223–230
DOI: 10.1007/s11665-010-9676-3

1059-9495/$19.00

Experimental Observations of Quasi-Static-Dynamic Formability in Biaxially Strained AA5052-O

Dahai Liu, Haiping Yu, and Chunfeng Li

(Submitted December 9, 2009; in revised form March 10, 2010)

To establish the efficacy of electromagnetically assisted sheet metal stamping (EMAS), a series of combined hydraulic bulging and electromagnetic forming (EMF) experiments are presented to evaluate the biaxial quasi-static-dynamic formability of an aluminum alloy (AA5052-O) sheet material. Data on formability are plotted in principal strain space and show an enhanced biaxial formability beyond the corresponding experimental results from conventional forming limit diagram. The plastic strains produced by the combined process are a little larger than or at least similar with those obtained in the fully dynamic EMF process. In addition, the biaxial forming limits of aluminum sheets undergoing both very low and high quasi-static prestraining are almost similar in quasi-static-dynamic bulging process. Limit formability seems to depend largely on the high-velocity loading condition as dictated by EMF. It appears that in quasi-static-dynamic forming, quasi-static loading is not of primary importance to the material's formability. Based on these observations, one may be able to develop forming operations that take advantage of this formability improvement of quasi-static-dynamic deformation. Also, this could enable the use of a quasi-static preform fairly close to the quasi-static material limits for the design of an EMAS process.

Keywords biaxial tension, electromagnetic forming (EMF), electromagnetically assisted sheet metal stamping (EMAS), quasi-static-dynamic formability

1. Introduction

Continuing pressure to reduce vehicle weight and emissions in automotive industry has caused many manufactures to substitute aluminum alloys for steels in applications that were formerly dominated by steel (Ref 1, 2). Unfortunately, the viability of the press forming of aluminum is hindered by the fact that aluminum has much lower formability compared with steel at room temperature. Efforts to obtain improved formability have led to renewed interest in high-velocity forming processes, among them electromagnetic forming (EMF).

Generally, the stamping parts are large and need very large electromagnetic energy input if using EMF to form the whole metal parts alone. Due to the practical limits of strength of tooling materials and the capacity of capacitor bank, the electromagnetic forces cannot be arbitrarily enlarged to form large parts. As a result, electromagnetically assisted sheet metal stamping (EMAS) (Ref 3-8) technique is being considered. EMAS, first referred to as the matched tool-electromagnetic (MT-EM) process (Ref 3, 4), combines the advantages of high-velocity EMF on forming aluminum alloys into the traditional sheet metal stamping process by means of embedding a set of electromagnetic coils in stamping tool halves. And in principle, both operations can be carried out in one nearly traditional press stroke (Ref 6, 7). Some experimental try-outs on this hybrid concept have been conducted and excellent improvement in formability of aluminum alloys has been observed (Ref 3-5, 8). The availability of experimental data is generally limited to verifying the feasibility of this concept, and as a result there are hardly any systematic discussions on the issues concerning the viability of EMAS process. Thus, studies on the fundamental material mechanics and plasticity must reveal an enhanced forming capability with the EMAS process to justify any further effort.

In essence, material response under a combined quasi-static-dynamic loading condition is the basic issue involved in an EMAS deformation process. To date, the deformation behaviors of materials have been extensively studied, not only under high strain-rate loading conditions, but also when the loadings are essentially quasi-static in nature. However, by the path dependency of plastic deformations, it would not be expected that the combined effect of static and dynamic deformations of a sheet material is symmetric or independent of application sequence. During complex strain paths, the plastic instability of metals presents some particular facets. In the quasi-static regime, the bulk of the investigations have been concerned with nonuniform deformation and early plastic instability in tension during reloading or after prestraining (Ref 9, 10), and a convincing argument has been presented that increasing the strain-rate would decrease the plastic strain at maximum load, and at localized necking prior to fracture. While under the high strain-rate (especially $>10^3$-10^4 s^{-1}) or high-velocity conditions, however, the results appear to be quite different and considerable evidence exists that an increase in strain-rate can result in an increase in the ductility of most metals, which is referred to as hyperplasticity (Ref 11-13). Whether these latter results are due to the influence of inertia or the strain history brought about by the forming process is still challenged (Ref 14), since many of the experiments were not directly designed to examine the influence of strain-rate or loading

Dahai Liu, Haiping Yu, and **Chunfeng Li**, School of Materials Science and Engineering, Harbin Institute of Technology, Harbin 150001, China. Contact e-mail: liudahai.hit@gmail.com.

history on the deformation process. And what is more, these high-velocity performances cited in the previous literature are almost entirely for fully dynamic deformations starting from flat blanks or uniform tubes with initial cold work state. The hybrid quasi-static-dynamic case, on the other hand, will be confounded by the various levels and distributions of prestrain introduced into the sheet material during the quasi-static initial forming stage of the process. Despite the fundamental mechanism of the extended ductility under high-velocity loading conditions, the apparent inconsistencies in the results obtained at the two loading rates have made the terminal behavior (fracture) of sheet in a quasi-static-dynamic deformation sequence be a disputable one. Some early work has summarized the changes in flow stress and terminal behavior brought by dynamic prestrain in a dynamic-static deformation sequence (Ref 15-17); however, little attempt has been made concerning the reverse sequence of deformations. Meyers (Ref 16) and Follansbee and Kocks (Ref 18) have investigated the change in constitutive behaviors resulting from the elevated strain rates from quasi-static region until the onset of the high-speed dynamic region, but unfortunately the studies were not directed to the terminal behavior of the solids. The only information on quasi-static-dynamic formability can be found in Vohnout's work (Ref 3) on plane-strain state, and a recently published work (Ref 19) on uniaxial tensile state.

With the issues mentioned above, the purpose of this study is to experimentally develop a basis from which the hybrid quasi-static-dynamic deformation and material response may be better understood and quantified. The biaxial-tension forming limits of an as-received aluminum alloy (AA5052-O) sheet are evaluated under a basic quasi-static-dynamic loading condition as dictated by the combined basic HBT and EMF experiments. The effect of quasi-static prestraining, through the acquisition of basic material formability data, is also assessed and discussed so as to provide an experimental evidence for the design of an EMAS process.

2. Experimental Procedure

2.1 Material

The material used in this investigation is commercially available AA5052-O sheet, 1 mm in thickness. The nominal chemical composition of the as-received material is Al-(2.2-2.8)Mg-0.25Si-0.4Fe-0.1Cu-0.1Mn-(0.15-0.35)Cr-0.1Zn (wt.%). This material was chosen for its usage as a potential substitute for steel for lightweight car body applications such as interior panels and components, truck bumpers, and body panels.

2.2 Methods

Based on the principle of EMAS, and to keep the hardware requirements simple, the hybrid quasi-static-dynamic experiments were conducted in two separate phases, quasi-static and dynamic (Ref 3, 19). The quasi-static and dynamic test procedures applied to the sheet samples were designed to restrict the sample deformation to biaxial expansion. Sheet samples were all first quasi-statically subjected to biaxial tension to specific prestrain levels using conventional hydraulic bulge apparatus, and then clamped in the coil fixture of the EMF system and dynamically loaded to failure.

A schematic of the hydraulic bulging system is shown in Fig. 1(a). The bulging of a sheet can be analyzed as a thin spherical shell expanded uniformly by an increasing hydrostatic internal pressure, where the meridional strain gradient is small at the periphery and quite large at the pole (Ref 20, 21). By increasing the hydrostatic internal pressure, a series of deformed shapes with different biaxial strain levels can be achieved. Specific strain levels can be described by measuring the dome height (h) using a displacement sensor, and can be reported through grid analysis. Accordingly, to designate the levels of prestraining, the limit dome height (h_m) was firstly determined where a failure was just about to occur, so that by selecting the appropriate dome height it was possible to vary the quasi-statically induced plastic strain at the top of the dome from zero to values close to where failure would occur.

Each sample after being quasi-statically bulged to the selected prestrained condition was then removed from the hydraulic bulging system and clamped in the coil fixture, as shown in Fig. 1(b), and dynamically loaded to failure. The EMF experiments were performed using an EMF system manufactured by Harbin Institute of Technology. This apparatus consists of six 120 μF capacitors each charged up 9.0 kV to provide total energy storage of about 30 kJ. The testing procedure is schematically shown in Fig. 1(b). A coil with a nearly spherical surface is used to deform the prestrained samples, which was wound to form a series of predetermined

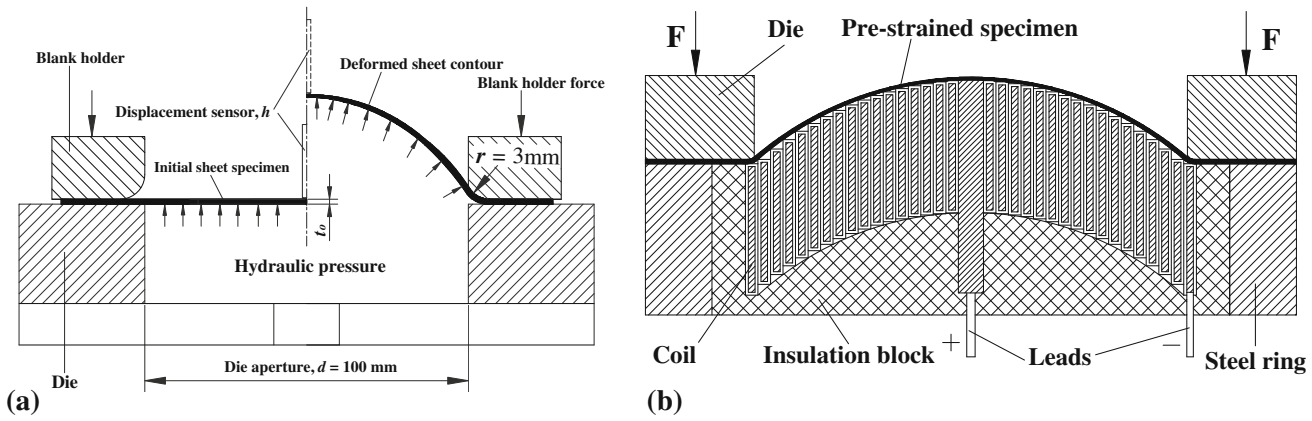

Fig. 1 Schematic of sample configuration: (a) quasi-static and (b) dynamic

contours matching to the quasi-statically prestrained samples, so that an efficient pulsed magnetic loading can be achieved to apply on the varied sample contour. The coil is mounted inside an insulation block, which is press-fit into a steel ring, serving the following dual purpose: as a constraint band for the coil, preventing its expansion, and as a flat lower binder for the sample being tested. A die with an open-round window of 100 mm in diameter and an entry radius of 10 mm to avoid tearing, also serves as an upper binder.

The AA5052-O sheets tested were cut into 180 mm × 180 mm squares. Circle grids of 2.5 mm in diameter were electrochemically etched into the material for strain measurements, which were conducted by using the CamSys, Inc. software ASAME Lite (Automated Strain Analysis & Measurement Environment) Version 4.1.

3. Results

3.1 Hydraulic Bulge Tests and Coil Determination

To evaluate the biaxial quasi-static forming limits of the as-received aluminum alloy, typical HBTs were conducted. Figure 2 shows a typical examined sample with a fracture in the pole region. In-plane strain pairs of the fracture zone were plotted on the traditional forming limit diagram (FLD) from a series of replicate samples, and were compared with the experimental FLD results determined by Hecker (Ref 22), as shown in Fig. 3. The differences in strains between replicate samples are within the accuracy of the ASAME measurement. As can be seen, nearly equi-biaxial tension strains are reported in HBT, and the biaxial limit strains agree closely with those obtained by Hecker. In addition, obtaining absolute equi-biaxial tension strains is almost impossible; the strain pairs from HBT provide reasonable insight into the biaxial quasi-static formability of the as-received aluminum.

An average dome height of 34.7 mm was measured from the fractured samples, which is then used as a reference that the prestrained states can be determined. Within this limit dome height, four groups of quasi-statically prestrained samples, labeled from no. 1 to 4 to identify strain levels varying from very little to values close to where failure would occur. The exact dome heights were measured using the displacement sensor. This is feasible for the deformation process is very slow (near static). The case without prestraining labeled with no. 0 is presented for comparison.

Figure 4 shows the prestrained samples and their average in-plane strain distributions are shown in Fig. 5(b), measured from grid analysis along the generatrix paths (Fig. 5a). For the axisymmetric characteristic of hydraulic bulging, strain distributions on the whole dome surface can be approximately described by the strain gradient along one meridian. As can be seen, strain levels at the pole region are higher than those at the periphery, typically for hydraulic bulging, in each grouped samples. Note the difference between major strain and minor strain are not very great at the pole, which indicates nearly equi-biaxial strain states, therefore, a quasi-static pre-straining level can be ascribed using the value of major prestrain.

To determine the shapes of coils used for dynamic re-deformation of each grouped pre-strained samples, the spherical assumptions of deformed sample in HBT were introduced in this work, which was analytically investigated

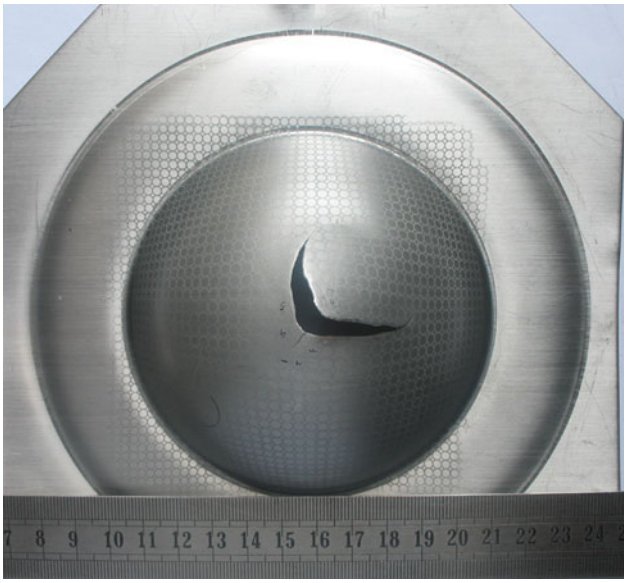

Fig. 2 Fractured sample using HBT

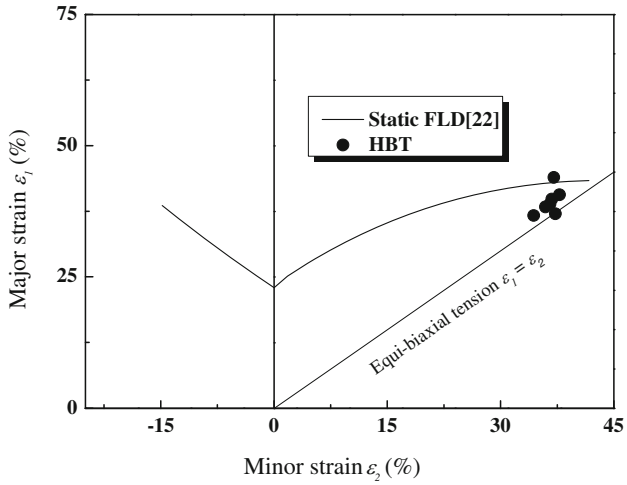

Fig. 3 Biaxial quasi-static forming limits from HBT

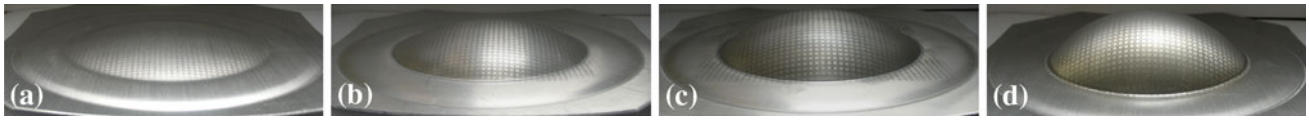

Fig. 4 Photographs of quasi-statically prestrained samples: (a) sample 1, (b) sample 2, (c) sample 3, and (d) sample 4

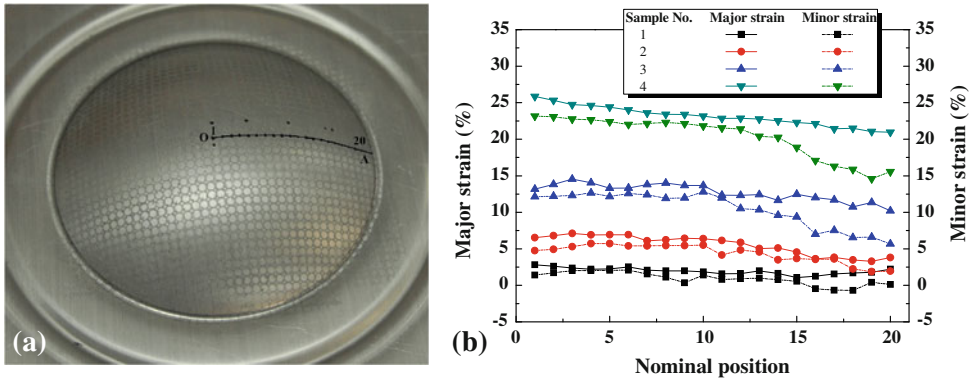

Fig. 5 Prestrain measurement in grouped samples: (a) positions for strain measurement and (b) strain distributions along O-A

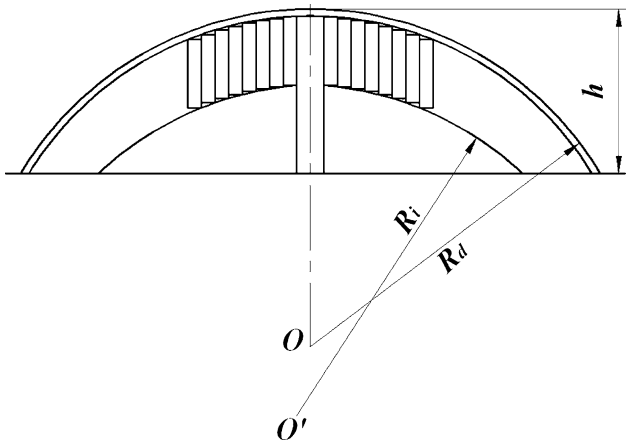

Fig. 6 Geometry schematic for coil determination

by Hill (Ref 20). By assuming that the prestrained dome is spherical and that there is a fillet in the cavity of the blank holder, the radius at the top of the dome can be analytically calculated:

$$R_{\mathrm{d}} = \frac{((d/2)+r)^2 + h^2 - 2rh}{2h}, \qquad \text{(Eq 1)}$$

where d is the diameter of the cavity, and h the dome height and r the fillet in the cavity of the blank holder. To match the profile of prestrained sample, the spherical coil was determined by uniformly arranging the turns along the inner surface of sample, as shown in Fig. 1(b). Assuming the wire of the coil has a rectangular cross section (30.4 mm × 1.4 mm in dimensions), a simple geometry relationship can be obtained from Fig. 6:

$$R_i = R_d - t, \qquad \text{(Eq 2)}$$

where R_i is the radius of insulation frame of coil (Fig. 1b), and t the thickness of blank. Accordingly, the coil geometry can be approximately determined by the dome height h. Thereby, four kinds of coil contours (No. C1-C4) matched to the prestrained samples were determined and designed, as shown in Fig. 7, in which the flat coil (No. C0) is also included. Table 1 summarizes the geometry details of the prestrained samples and its determined coils.

Table 1 Geometry details for prestrained samples and coils

Sample no.	Average dome height h, mm	Analytical dome radius R_{d}, mm	Relevant coil no.	Coil turns	Radius of coil R_i, mm
0	0	···	C0	14	···
1	8.86	165.99	C1	14	165.0
2	15.29	100.00	C2	14	99.0
3	21.92	74.47	C3	14	73.47
4	30.41	60.15	C4	14	59.15

3.2 Quasi-Static-Dynamic Formability

The EMF bulging of the grouped samples with varying prestrains were conducted using the 14-turn coils (Fig. 7) to assess the biaxial hybrid quasi-static-dynamic formability of the as-received AA5052-O. Here, the fully dynamic phenomenon, for which the flat coil (No. C0) is used to deform the samples (No. 0) without prestraining, is also considered to be a special case of hybrid quasi-static-dynamic deformation.

For each group of samples (specified in Table 1), the initial approach was to define the minimum energy of discharge needed to neck or fracture the blank. To define this level, we incrementally increased the energy in the capacitors by adjusting the charging voltage. Figure 8 shows the obtained safe, necked and fractured parts. The process resulted in a distinctive dome shape, which is due to the magnetic pressure distributions (Ref 23). One of the issues encountered in EMF re-deformation of this class of samples is fracture in the area near the die-entry radius, as shown in Fig. 9. The failure in this location is due to high strains caused by high-strain gradients at the tangency point between sheet and die due to frictional forces at the die. This behavior is common in conventional press forming of hemispherical dome samples. However, this kind of fracture is not expected to elucidate the biaxial forming limits due to insufficient deformation of sheet dome. Using grease in the area near the die-entry radius may be helpful, and a typical fracture in the pole region can accordingly be produced (Fig. 8c). Table 2 summarizes the launch details of the samples used for failure strain analysis for five grouped aluminum sheets.

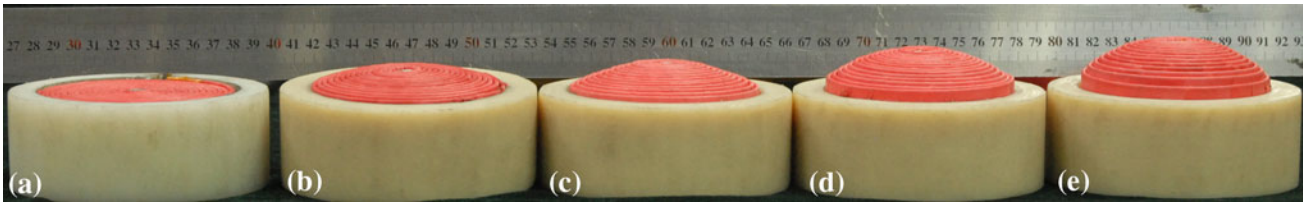

Fig. 7 Configurations of the coils used in this study: (a) flat coil C0, (b) coil C1, (c) coil C2, (d) coil C3, and (d) coil C4

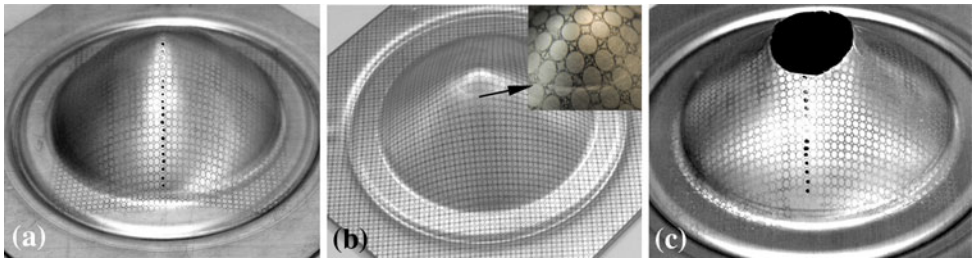

Fig. 8 Typical states of deformed samples: (a) safe, (b) necking, and (c) fracture

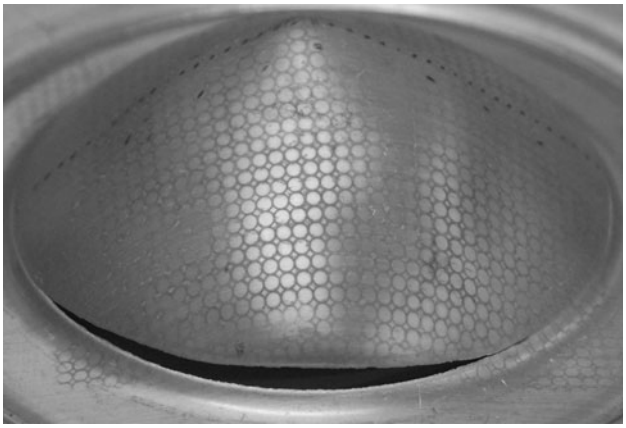

Fig. 9 Sample fractured in the area near die-entry radius

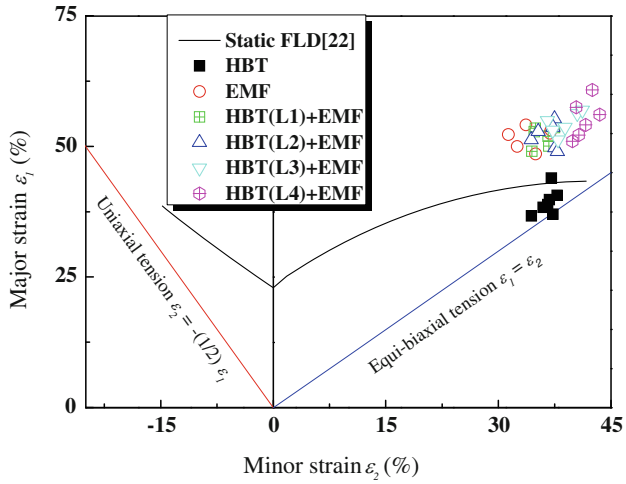

Fig. 10 Results on formability of AA5052-O

Table 2 Launch details for samples selected for failure strain analysis

Sample no.	Launch energy, kJ	Failure	Lubrication	For strain analysis
0	15.21/6.5 kV	Necking/pole region	None	Yes
	17.64/7.0 kV	Necking/pole region	None	Yes
	20.25/7.5 kV	Fracture/pole region	With grease	Yes
1	15.21/6.5 kV	Fracture/die-entry	None	No
	17.64/7.0 kV	Fracture/pole region	With grease	Yes
	20.25/7.5 kV	Fracture/pole region	With grease	Yes
2	12.96/6.0 kV	Fracture/die-entry	None	No
	17.64/7.0 kV	Fracture/pole region	With grease	Yes
	20.25/7.5 kV	Fracture/pole region	With grease	Yes
3	11.90/5.75 kV	Fracture/die-entry	None	No
	12.96/6.0 kV	Fracture/pole region	With grease	Yes
	15.21/6.5 kV	Fracture/pole region	With grease	Yes
4	10.89/5.5 kV	Fracture/die-entry	None	No
	11.90/5.75 kV	Fracture/pole region	With grease	Yes
	15.21/6.5 kV	Fracture/die-entry	With grease	No

With the approaches mentioned above, we obtained the formability results shown in Fig. 10. Strain pairs from circle grid analysis were plotted on the traditional FLD, and the comparison with the experimental quasi-static FLD results determined by Hecker was also made. Strains on quasi-statically formed sample conforms relatively well to the published FLD, whereas the quasi-static-dynamic samples withstand much higher biaxial strains beyond quasi-static forming limits, which, as expected, conveys the extent of improvement in formability quite clearly. Despite the introduction of quasi-static prestraining, all the hybrid-forming samples convey the extended forming limits over the quasi-static case consistently. And what is more, the present study also considers the free expansion experiments under absolute high-velocity EMF loading conditions. Other researchers (Ref 23-26) have conducted similar experiments on free forming of different aluminum alloys. Oliveira and Worswick (Ref 24) and Oliveira et al. (Ref 25) considered forming aluminum sheet into a rectangular die opening. No formability improvement in their electromagnetically free-formed parts was reported. Those authors showed EMF strains higher than the quasi-static forming limits but attributed them to strain path changes after workpiece failure. However, Imbert et al. (Ref 23) and Golovashchenko (Ref 26) did show EMF free-forming strains above the traditional quasi-static limits of their aluminum alloy on safe (no necking or fracture) parts (Ref 23) and fracture parts (Ref 26). Those experiments also used aluminum sheet free formed into a circular die opening and indicated that EMF may enhance free formability. Compared with these experiments mentioned above, a much more significant improvement in formability is observed in this study. This is probably for the reasons that much higher strain rates are achieved by altering the boundary conditions to make the dome fractured in the pole region, not the die-entry region, and the aluminum alloy used in these earlier experiments was AA5754, which is considerably different from our alloy AA5052-O. Studies by Vural et al. (Ref 27) and Yadav et al. (Ref 28) showed a distinct alloy-dependent threshold above which strain-rate sensitivity becomes important, indicating these differences may significantly influence the experiments.

3.3 Effect of Quasi-Static Prestrain

Much different from a fully dynamic process, the effect of quasi-static prestrain is introduced in a quasi-static-dynamic forming process. To further evaluate the effect of quasi-static prestraining, the combined strain state was carefully examined from an exact pre-straining state. This was done by tracking the deformation path of a specific circle grid etched on the sheet surface. For failures often occur near the pole region (Fig. 8b and c) and the difference of in-plane prestrain pairs here are relatively uniform (Fig. 5b), the major prestrain is specified as the reference of prestraining level, against of which, the ultimate hybrid strains pairs were plotted, as shown in Fig. 11, for each grouped samples. Here we also include the fully dynamic case as a special hybrid-forming process.

Figure 11 demonstrates a slight increase of the limit strains as a function of increasing major prestrain level. It is interesting to compare the measured formability for the five grouped samples studied. They are quite different with biaxial quasi-static prestraining levels ranging between 0% and 25% (recall the major prestrain increases from Sample No. 0-4). Although there are large differences in their quasi-static prestraining

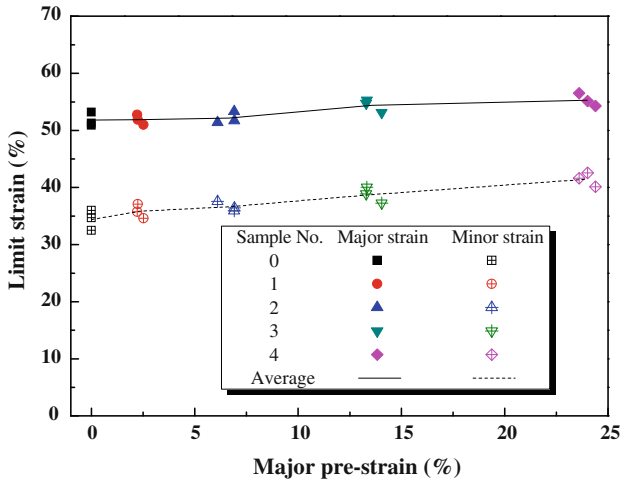

Fig. 11 Relationship between prestrain and limit strains

levels, such is not the case with the total limit strains of these samples. All the points for biaxial quasi-static-dynamic formability data lies approximately in the 48-56% (major strain) and 32-43% (minor strain) strain ranges. There is not a lot of difference in the maximum strains that can be obtained from the low versus high quasi-static prestrained samples. For example, Sample No. 4 has the highest quasi-static prestraining level of about 24%, very close to quasi-static material limits, from the chosen samples. It also has the highest ultimate formability, but it is within the scatter of the other grouped samples. The highest "hybrid-forming" strain point obtained with this sample is approximately (0.41, 0.56). On the other hand, Sample No. 0 (the fully dynamic EMF case) has the lowest quasi-static prestraining level of 0% from the chosen samples. The highest "hybrid-forming" strain point obtained with this sample is approximately (0.34, 0.52). Thus in spite of a huge difference (ranging from 0% to value close to quasi-static limits) in the quasi-static prestraining of Sample No. 0 and 4, their quasi-static-dynamic formability is not appreciably different. In addition, the results show the quasi-static prestraining seems to have little effect on the total plastic strains, and also at least seems to play a synergistic role in the total quasi-static-dynamic plastic deformation process, also indicated by the previous literature (Ref 3, 4, 19). And the hyperplasticity effect of quasi-static-dynamic deformation appears mainly depended on the high-velocity loading conditions.

4. Comments and Discussion

The preliminary hydraulic bulging-EMF experiments performed in this study have been shown to support the fundamental premise for the utility of the EMAS process. Experimental results indicate that the two component processes, quasi-static bulging and high-velocity bulging, have a synergistic effect on total plastic deformation of the as-received aluminum alloy sheet. The formability produced by the combined process is larger than that produced by either component process. The data are not sufficient to attempt a formulation of any basic constitutive relation, but will be presented in a manner that is deemed conducive to providing

insight about the material behavior during an EMAS process to an application engineer.

Of particular note, where quasi-static-dynamic forming follows a total plastic deformation pattern very similar to the fully dynamic EMF case, one can conclude that quasi-static prestraining plays a very limited role in the fracture process, and the high-velocity EMF accounts for the enhanced formability of quasi-static-dynamic deformation. However, much different from the typical EMF process, the high-velocity responses in quasi-static-dynamic process will be confounded by the various levels and distributions of quasi-static prestrain introduced into the sheet material during the quasi-static initial forming stage of the process. A question that naturally follows is whether the introduction of prestraining would affect the ultimate formability of sheet material, which is crucial in establishing the efficiency of EMAS. From the issues mentioned in Section 1, the direct effect of the existing prestrain is that the fully work-hardened aluminum sheets are not expected to perform as well as a lightly worked condition. However, experimental evidence in this work seems to have challenged this assumption. The introduction of quasi-static prestraining will not weaken the total formability during quasi-static-dynamic deformation. This would provide meaningful information for the design implication for the EMAS process that greater overall formability may be achieved by pushing the preform fairly close to the quasi-static material limits.

Extensive investigations have suggested that dynamic formability would increase for inertia stabilization effect (Ref 11-13, 29, 30), tool/sheet impact effect (Ref 23, 31), or changes in constitutive behavior (Ref 18, 32) during high-velocity deformation, and there is also some experimental evidence that increasing sample size (Ref 33) and sheet thickness (Ref 34). However, the results from these experiments do not provide enough resolution to shed much light on this special issue encountered in EMAS technique. Till now, the fundamental mechanism of high velocity is still the subject of considerable debate and needs further investigation (Ref 6, 14).

5. Conclusions

1. Biaxial formability of AA5052-O sheet can be significantly improved by using the concept of hybrid quasi-static-dynamic deformation. The biaxial quasi-static-dynamic forming limits are much higher than those obtained in quasi-static bulging, and are at least as good as those shown in the fully dynamic EMF process. This is confirmed by preliminary experiments of hydraulic bulging and EMF results.
2. Despite the introduction of quasi-static deformation, the total formability of as-received aluminum alloy sheet seems to be mainly determined by the high-velocity deformation process. A similar hybrid-formability can be observed with varying quasi-static prestraining levels.

Acknowledgment

The authors would like to express their sincere appreciation for the financial support of the National Science Foundation of China (Grant no. 50805036).

References

1. M. Satio, S. Iwatsuki, and K. Yasunaga, Development of Aluminum Body for the Most Fuel Efficient Vehicle, *JSAE Rev.*, 2000, **21**(1), p 511–516
2. M. Bull, R. Chavali, and A. Mascarin, "Benefit Analysis: Use of Aluminum Structure in Conjunction with Alternative Powertrain Technologies in Automobiles," Research report, IBIS Associates, Inc. for the Aluminum Association, 2008
3. V.J. Vohnout, "A Hybrid Quasi-Static/Dynamic Process for Forming Large Sheet Metal Parts from Aluminum Alloys," Ph.D. Thesis, The Ohio State University, The Ohio State, 1998
4. V.J. Vohnout, G.S. Daehn, and R. Shivpuri, A Hybrid Quasi-Static-Dynamic Process for Increased Limiting Strains in the Forming of Large Sheet Metal Aluminum Parts, *Proceedings of the Sixth ICTP*, Nuremberg, 1999, p 1359-1364
5. G.S. Daehn, J.H. Shang, and V.J. Vohnout, *Electromagnetically Assisted Sheet Forming: Enabling Difficult Shapes and Materials by Controlled Energy Distribution*, Energy Efficient Manufacturing Processes, USA, TMS, 2003, p 117-128
6. G.S. Daehn, V.J. Vohnout, and S. Datta, Hyperplastic Forming: Process Potential and Factors Affecting Formability, *Mater. Res. Soc. Symp. Proc.*, 2000, **601**, p 247–252
7. V.J. Vohnout and G.S. Daehn, Reducing Stamped Part Development Time with Pulsed Energy Assistance, www.osu.edu/hyperplasticity, 2004
8. J.H. Shang, "Electromagnetically Assisted Sheet Metal Stamping," Ph.D. Thesis, The Ohio State University, The Ohio State, 2006
9. A. Graf and W. Hosford, The Influence of Strain-Path Changes on Forming Limit Diagrams of Al 6111 T4, *Int. J. Mech. Sci.*, 1994, **36**(10), p 897–910
10. J.V. Fernandes, L.F. Menezes, D.M. Rodrigues et al., Non-Uniform Deformation After Prestrain, *Eur. J. Mech. A/Solid*, 2000, **19**, p 209–221
11. V.S. Balanethiram and G.S. Daehn, Enhanced Formability of Interstitial Free Iron at High Strain Rates, *Scripta Metall. Mater.*, 1992, **27**, p 1783–1788
12. V.S. Balanethiram and G.S. Daehn, Hyperplasticity: Increased Forming Limits at High Workpiece Velocity, *Scripta Metall. Mater.*, 1994, **30**, p 515–520
13. V.S. Balanethiram, X.Y. Hu, M. Altynova et al., Hyperplasticity: Enhanced Formability at High Rates, *J. Mater. Process. Technol.*, 1994, **45**, p 595–600
14. M. Seth, "High Velocity Formability and Factors Affecting It," Ph.D. Thesis, The Ohio State University, The Ohio State, 2006
15. A.A. Ezra, *Principles and Practices of Explosive Metalworking*, Industrial Newspapers Limited, London, England, 1973
16. M.A. Meyers, *Dynamic Behavior of Metals*, Wiley, New York, 1994
17. I.M. Fyfe and A.M. Rajendran, Dynamic Pre-Strain and Inertia Effects on the Fracture of Metals, *J. Mech. Phys. Solids*, 1980, **28**, p 17–26
18. P.S. Follansbee and U.F. Kocks, A Constitutive Description of the Deformation of Copper Based on the Use of the Mechanical Threshold Stress as an Internal State Variable, *Acta Metall.*, 1988, **36**(1), p 81–93
19. C.F. Li, D.H. Liu, H.P. Yu et al., Research on Formability of 5052 Aluminum Alloy Sheet in a Quasi-Static-Dynamic Tensile Process, *Int. J. Mach. Tools Manuf.*, 2009, **49**, p 117–124
20. R. Hill, A Theory of the Plastic Bulging of a Metal Diaphragm by Lateral Pressure, *Philos. Mag. Ser 7*, 1950, **41**(322), p 1133–1142
21. M. Atkinson, Accurate Determination Biaxial Stress-Strain Relationships Form Hydraulic Bulging Tests of Sheet Metals, *Int. J. Mech. Sci.*, 1997, **39**(7), p 761–769
22. S.S. Hecker, Formability of Aluminum Alloy Sheets, *J. Eng. Mater. Technol. Trans. ASME*, 1975, **97H**, p 66–73
23. J.M. Imbert, S.L. Winkler, M.J. Worswick, and D.A. Oliveira, The Effect of Tool-Sheet Interaction on Damage Evolution in Electromagnetic Forming of Aluminum Alloy Sheet, *J. Eng. Mater. Technol.*, 2005, **127**, p 145–153
24. D.A. Oliveira and M.J. Worswick, Electromagnetic Forming of Aluminum Alloy Sheet, *J. Phys. IV Fr.*, 2003, **110**, p 293–298
25. D.A. Oliveira, M.J. Worswick, M. Finn, and D. Newman, Electromagnetic Forming of Aluminum Alloy Sheet: Free-Form and Cavity Fill Experiments and Model, *J. Mater. Process. Technol.*, 2005, **170**, p 350–362

26. S.F. Golovashchenko, Material Formability and Coil Design in Electromagnetic Forming, *J. Mater. Eng. Perform.*, 2007, **16**(3), p 314–320
27. M. Vural, D. Rittel, and G. Ravichandran, "High Strain Rate Behavior of Metal Alloys at Large Strains," GALCIT report, Graduate Aeronautical Laboratories, The California Institute of Technology, Pasadena, CA, 2004
28. S. Yadav, D.R. Chichili, and K.T. Ramesh, The Mechanical Response of a 6061-T6 Al/Al_2O_3 Metal Matrix Composite at High Rates of Deformation, *Acta Metall. Mater.*, 1995, **43**(12), p 4453–4464
29. N.J. Sorenson and L.B. Freund, Unstable Neck Formation in a Ductile Ring Subjected to Impulsive Radial Loading, *Int. J. Solid Struct.*, 2000, **37**, p 2265–2283
30. K. Nilsson, Effects of Inertia on Dynamic Neck Formations in Tensile Bars, *Eur. J. Mech. A/Solid*, 2001, **20**, p 713–729
31. M. Seth, V.J. Vohnout, and G.S. Daehn, Formability of Steel Sheet in High Velocity Impact, *J. Mater. Process. Technol.*, 2005, **168**, p 390–400
32. G. Regazzoni, U.F. Kocks, and P.S. Follansbee, Dislocation Kinetics at High Strain Rates, *Acta Metall.*, 1987, **35**(12), p 2865–2875
33. A. Tambane, M. Altynova, and G.S. Daehn, Effect of Sample Size on Ductility in Electromagnetic Ring Expansion, *Scripta Mater.*, 1996, **34**(8), p 1345
34. V.B. Shenoy and L.B. Freund, Necking Bifurcations During High Strain Rate Extension, *J. Mech. Phys. Solids*, 1999, **47**, p 209